JACS
JOURNAL OF THE AMERICAN CHEMICAL SOCIETY

Article

pubs.acs.org/JACS

Thermoelectric Efficiency of Organometallic Complex Wires via Quantum Resonance Effect and Long-Range Electric Transport Property

Hisao Nakamura,*[,†] Tatsuhiko Ohto,[†] Takao Ishida,[‡] and Yoshihiro Asai[†]

[†]Nanosystem Research Institute (NRI), "RICS", Advanced Industrial Science and Technology (AIST), 1-1-1 Umezono, Tsukuba, Ibaraki 305-8568, Japan

[‡]NRI, AIST, 1-2-1 Namiki, Tsukuba, Ibaraki 305-8564, Japan

Supporting Information

ABSTRACT: Superior long-range electric transport has been observed in several organometallic wires. Here, we discuss the role of the metal center in the electric transport and examine the possibility of high thermoelectric figure of merit (ZT) by controlling the quantum resonance effects. We examined a few metal center (and metal-free) terpyridine-based complexes by first-principles calculations and clarified the role of the metals in determining the transport properties. Quasi-resonant tunneling is mediated by organic compounds, and narrow overlapping resonance states are formed when d-electron metal centers are incorporated. Distinct length (L) and temperature (T) dependencies of thermopower from semiconductor materials or organic molecular junctions are presented in terms of atomistic calculations of ZT with and without considering the phonon thermal conductance. We present an alternative approach to obtain high ZT for molecular junctions by quantum effect.

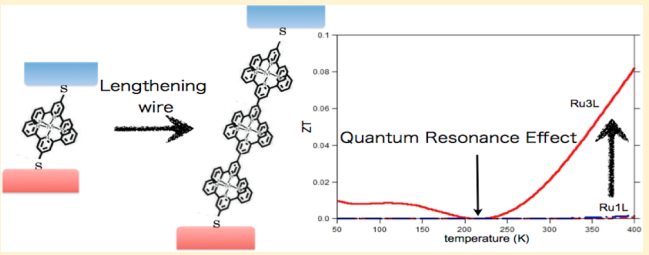

1. INTRODUCTION

Organic molecular compounds are promising materials for designing tailored functional devices.[1,2] A rich accumulation of data on chemical modification and synthesis techniques is available, and molecular orbital (MO) engineering sheds new light on designing electric and energy conversion devices.[3−6] Thermoelectricity of molecular junctions has been extensively investigated to understand the quantum energy conversion as well as electric and thermal transport processes. Papadopoulos et al. showed that the nodal structure of the electric transmission coefficient appeared by attaching side groups to a carbon backbone, and demonstrated that the nodal profile is a result of the Fano resonance.[7] Finch et al. argued that a giant Seebeck coefficient (S_e) is achievable by controlling the Fano resonance.[8,9] Similar approaches to enhance S_e were proposed by several research groups such as π cross-conjugated molecules by Ratner's group[10] or π ring molecules with asymmetrically positioned anchors by Ke et al.[11] All of the above approaches are based on quantum interference effects between a dominant tunneling orbital (conducting orbital) and localized states. Because thermal conductance is suppressed by mismatching of phonon density of states (DOS) between electrodes and molecules, high figure of merit (ZT) seems to be expected. However, a few problems exist in the above argument. First, the electric conductance (σ) of tunneling systems often exponentially decreases as a function of the wire length (thickness of film) L, that is, $\sigma \propto \exp(-\beta L)$.[12] A sufficient distance between the hot and cold electrodes is necessary to keep a temperature (T) gradient, while the exponential decrease in the electric conductance rapidly reduces the thermoelectric efficiency. Second, controlling the position of Fano resonances is difficult, which must be close to the Fermi level (E_F). Controlling the resonance will strongly depend on the chemical nature of the backbone and side groups as well as on the molecular conformation. The use of gate voltage or electrochemical control can be an alternative strategy; however, it is not practical at the present stage.

In this study, we performed a theoretical analysis of the coherent transport process in organometallic complexes and discussed its thermoelectric properties. Our findings offer two potential advantages provided by organometallic molecular junctions to tackle the difficulties of molecular thermoelectric devices. The first is that the suppression of the rapid decrease of ZT by lengthening the wire is possible because of the coexistence of the small β and mismatching of phonon DOS. Recently, several research groups have shown that superior long-range electric transport can be realized by nanowires or self-assembled monolayers of metal-based redox-active center molecules such as organometallic complexes.[13−17] There is a lot of scope for understanding superior long-range transport mechanism, that is, whether the coherence is kept in the entire long wire or the hopping mechanism is dominant by strong electron-localization and electron−phonon interactions. How-

Received: July 30, 2013

   dx.doi.org/10.1021/ja407662m | J. Am. Chem. Soc. XXXX, XXX, XXX−XXX

ever, very recent studies show that a small β (10^{-2}–10^{-3} Å^{-1}) is possible by coherent transport within a 10-nm scale for several organometallic systems. In the present calculations, we adopted terypyridine-based complex systems and reproduced the same order of magnitude for β. We found that narrow overlapping resonance states were formed by incorporating d-electron metal centers such as Ru. Moreover, we observed the enhancement of S_e or violation of the Wiedemann–Franz (WF) law by narrow overlapping resonance effect. Jaggy transmission coefficient is roughly controllable only by an increasing number of complex molecular units because each unit has a few quasi-degenerated frontier orbitals that interact with each other. The above-mentioned electric properties suggest an alternative quantum interference effect to improve ZT, that is, lengthening the organometallic wire instead of introducing side-group chemical modifications. Here, we present first-principles results and a detailed analysis of the length and temperature dependence of ZT, in which the effect of the phonon thermal transport was included. Hereafter, we use the atomic unit ($e = \hbar = 1$).

2. ELECTRIC TRANSPORT OF ORGANOMETALLIC COMPLEXES

Long-range electric transport has been reported for several organometallic molecular wires in which Zn, Fe, Co, and Ru centers were incorporated into organic compounds such as oligo-porphyrin,[15] bis(terpyridine),[17] ap4,[18] and bis(σ-arylacetylide).[13] The measured β values of bis(terpyridine)-based Fe and Co complexes are 2.28×10^{-2} and 1.00×10^{-3}, respectively.[17] Recently, Terada et al. reported $\beta \approx 1.00 \times 10^{-2}$ Å^{-1} for a Ru complex multilayer film[16] in which the unit was terpyridine–phenyl–terpyridine. The measured β values were only 1/10–1/100 of those of standard organic molecular junctions; that is, the superior long-range electric transport is realized by incorporating metal centers. A quasi-resonant coherent tunneling mechanism involving the metal center triggering the formation of resonance states was suggested.[16]

Generally, two charge migration mechanisms are considered to analyze the electric transport of molecular junctions. One is the coherent (ballistic) transport, and the other is the thermally induced hopping (TIH) mechanism. It is difficult to identify the mechanism that is dominant without the simultaneous measurement of temperature and length dependencies. Furthermore, an electron wave function can be delocalized within several molecular units with the electron hopping between these moieties. The temperature dependence of σ and thermal activation energy, E_a, are important criteria to understand the transport mechanism.[19] The dominant mechanism responsible for small β and scale of coherent length of organometallic molecular wires is still being debated. Recently, Sedghi et al. reported that E_a of σ-oligo-porphyrin is much smaller than that of standard organic molecular wires. They found that E_a increases by lengthening the wire. This behavior is opposite to the temperature dependence of E_a expected according to the small polaron theory, and they concluded that the transport is coherent (direct) tunneling.[15] The temperature dependence of a terpyridine-based Ru complex was measured by Terada et al. with E_a being $\sim 10^{-3}$ eV in low-temperature regime.[16] While E_a becomes $\sim 10^{-2}$ eV in the room-temperature regime, the value is still so small that σ is almost temperature-independent. In other words, the electron–phonon coupling strength is sufficiently weak. Furthermore, recent theoretical calculations by weak coupling theories such as lowest-order Born expansion or self-consistent Born approximation have predicted that inelastic current is $\leq$10% of the ballistic current for low-conductance systems in the room-temperature regime.[20,21] Hence, we conclude that a theoretical analysis omitting the electron–phonon interaction is reasonable as the first approximation.

The prime focus is to discuss small β and quantum resonance effect on ZT in organometallic complexes rather than verifying individual experimental results. To avoid a huge computational task and to determine the molecular conformation and transport property, we introduced simplified organometallic wires as model systems while adopting the same terpyridine group previously used[16,17] as a prototype organic compound. The introduced system is illustrated in Figure 1. The adopted molecular unit consists of bis(terpyridine) and a metal center labeled M, henceforth called an "M-complex". Each M-complex is directly connected to lengthen the organometallic wire, even though several linkers such as ethylene,[15] phosphonic acid,[16] and phenyl[17] moieties were examined in the experiments. The most simple anchors were selected for our model; that is, the wire was anchored to Au(001) electrodes by thiol atoms. We adopted M such that it contained transition metals and "metal-free" as metal centers, that is, Ru (d-electron metal), Cu (s-electron metal), and Vac [no metal in the bis(terpyridine) unit]. Superior long-range transport has been observed for organic compounds, including d-electron transition metal complex such as Ru; however, there is no clear observation of long-range transport for s-electron transition metal complexes. Therefore, theoretical calculations of the above three M complexes will provide detailed contribution of the metal centers to small β. In addition, we calculated the β value of the Fe complex. We lengthened the wire to three units and referred to them as M1L, M2L, and M3L, indicating that the wire consisted of one, two, and three molecular units, respectively. The structures were determined by spin-polarized density functional theory (DFT). The calculated dihedral angle

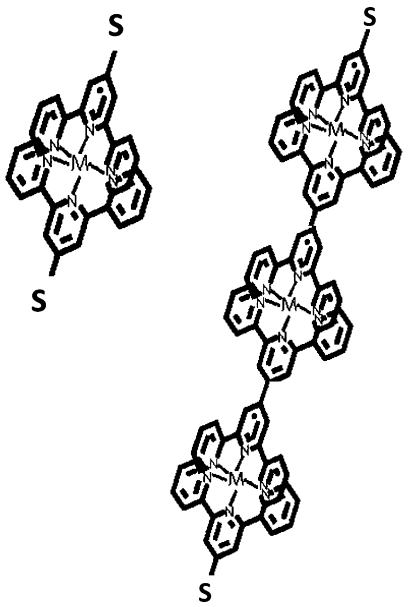

Figure 1. Chemical structures of the M complex wires connected to the Au(001) electrodes. The left and right panels show one (1L) and three (3L) organometallic molecular units, respectively. The label M at the center of terpyridine represents Vac (metal-free), Cu, or Ru atoms. The anchor atom is an S atom.

dx.doi.org/10.1021/ja407662m | J. Am. Chem. Soc. XXXX, XXX, XXX–XXX

between the molecular planes of the adjacent terpyridines was ~30° as a result of the direct connection of the neighboring terpyridine units. The length of the complex molecular unit was ~10.9 Å for all of the systems. The existence of a metal center or dependence of metal species did not alter the molecular conformation and wire length (length <0.2 Å).

3. RESULTS AND DISCUSSION

3.1. Long-Range Electric Transport and Narrow Overlapping Resonances. The electric transport properties were calculated by the nonequilibrium Green's function (NEGF) method.[22−25] Conductance of the Vac complex wire is lower than 10^{-8} G_0 when the wire consists of more than two Vac complex units (Vac2L). By incorporating a Cu atom, the conductance values of Cu1L, Cu2L, and Cu3L become large enough to evaluate β. The resulting plot is illustrated in Figure 2, and the obtained β is 0.34 Å^{-1}, which is of the same order as

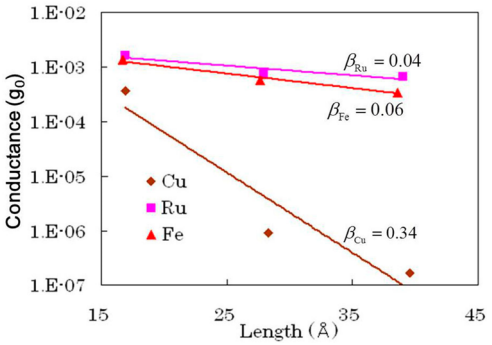

Figure 2. Log plots of conductance as a function of length and linear fittings for M complex wires, where M is Cu (◆), Ru (■), and Fe (▲). The conductance values at the zero temperature limit were used for plotting. The temperature dependence of conductance does not change the order of β of each metal center.

that of a standard organic molecular wire. On the contrary, the incorporation of a Ru atom drastically reduces β. The calculated β is 4.00×10^{-3} Å^{-1} for Ru complex wire (Figure 2). Our result reasonably agrees with β reported in the previous experimental studies; however, several other anchor units or linkers were used. We checked the temperature dependence of β to account for the temperature factor of the Fermi distribution. This temperature dependence is sometimes important when the transport is resonant tunneling and the sharpness of the isolated resonance peak is close to the derivative of the Fermi distribution function.[15] We calculated β by varying the electronic temperature from 100 to 300 K for the Ru complex. The obtained β value is less than 7.50×10^{-2} Å^{-1} over the entire temperature range, although the largest deviation from β at $T = 0$ K was observed at $T \approx 200$ K. Thus, we confirmed that, by using first-principles calculations, superior long-range transport by direct tunneling (not TIH) is possible and that the exponent factor β strongly depends on the metal species.

To verify the role of the metal center, we calculated the local electric current vectors, which are defined as the nonequilibrium bond-current on each atom[26,27] (Figure 3). The magnitude of the bond-current is represented by the brightness, and it is normalized for each system. The vectors whose (normalized) current density are lower than 0.2 are not plotted to show the role of metal to tunneling path. From the definition, the sum of influx and outflux of bond-current is zero when the total charge in the device region is conserved. In the

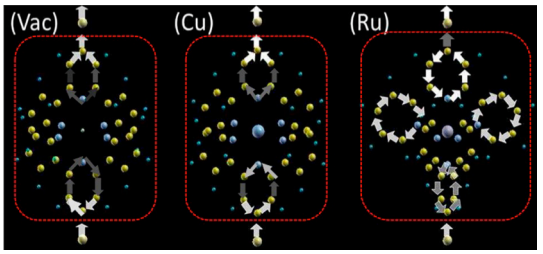

Figure 3. Local current vectors in the Vac, Cu, and Ru complex. The magnitude of the current density on each atom is represented by the brightness of the arrow (i.e., the brighter are the arrows, the larger is the current intensity). The current intensity is normalized, the maximum intensity is set to unity for each system, and magnitudes smaller than 0.2 are not presented.

present calculation, the current vectors were estimated by low-bias limit approximation as shown in the Supporting Information, and the charge was conserved within reasonable numerical accuracy. The Vac and Cu complex have a considerably small local electric current on all atoms. On the contrary, clear bond-currents on the terpyridine rings were found in the Ru complex; that is, the tunneling electron passes through the terpyridine rings. It is also notable that no local electric current vector was found on Ru atoms. This result contradicts the inference that quasi-resonant tunneling is mediated by a metal center. To clarify the role of the metal center and carbon backbone separately, we calculated the site-energy alignment. The quantitative site-energy alignment can be obtained by a first-principles molecular projected state Hamiltonian (MPSH), in which the energy-shifting and broadening of the spectra by coupling with the outer region are included by effective Hamiltonian formalism.[28] We defined the sites by dividing each M complex into chemical subgroups, for example, anchor (thiol atom), terpyridine moieties, and metal centers. Because the site energies depend on the spin components, we selected those of the major spin state. Here, the major spin state is defined as the component giving the largest conductance. The resulting site-energy diagrams are shown in Figure 4, where E_F is set to zero. In the Vac complex wire, the site energies of the terpyridine groups are aligned along the energy level ~1.5 eV above the E_F. Because the transfer integrals between the terpyridine moieties are much

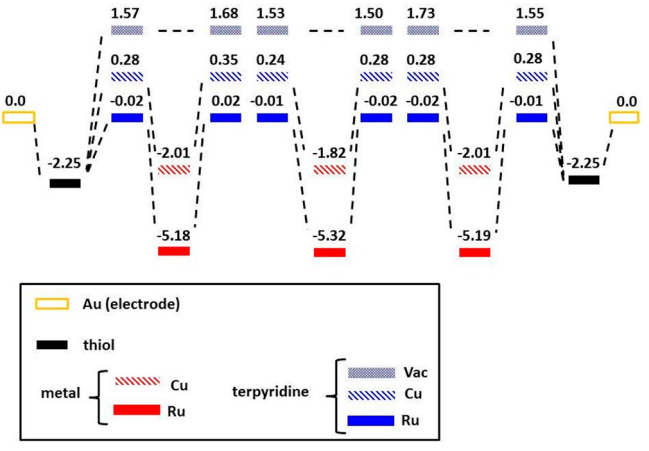

Figure 4. Site-energy diagrams for each group of Vac3L, Cu3L, and Ru3L wires. The Fermi level of the electrode is set to zero, and the site energies are given in eV. Inset: Site symbols.

dx.doi.org/10.1021/ja407662m | J. Am. Chem. Soc. XXXX, XXX, XXX−XXX

smaller than 1.5 eV, the tunneling is completely off-resonant and has approximately zero conductance. Here, we briefly comment that the site-energy levels of the terpyridine groups relating to tunneling are higher than E_F. This is consistent with the recent theoretical analysis that the tunneling electron of pyridine systems passes through the lowest unoccupied molecular orbital (LUMO), and it has also been experimentally confirmed.[29−31] Despite overestimating the absolute value of the conductance, NEGF-DFT provides reasonable results of the relative values of conductance and is useful to analyze universal transport properties.[32] Therefore, the DFT error does not seriously affect our discussion. The correction of the highest occupied molecular orbital (HOMO)-LUMO gap by GW approximation, etc., is required for a more quantitative analysis of the experimental observations,[33−35] while such quantitative analysis is out of our purpose.

By inserting metal centers, the site-energy alignment rapidly changes. When Cu is incorporated, the site energy of Cu had a value (−2.00 eV) similar to the difference between the Cu ionic potential and the work function of an Au electrode (∼ −2.25 eV). The site-energy level of Cu is considerably low to mediate resonant tunneling. However, energy levels of the terpyridine sites shift down (∼1.30 eV) to E_F as compared to those in the Vac complex. By replacing the metal center from Cu to Ru, the terpyridine energy level lowers by more than 1.60 eV, and the energy difference from E_F is only 0.03 eV. On the contrary, the site-energy level of Ru (−5.18 eV) is much lower than that of the Cu, even though the ionic potentials of Cu and Ru are comparable. These MPSH analyses suggest that the site-energy alignment is influenced by the metal center, and the path of tunneling is terpyridine (organic compound) groups. The metal species dependence of β relates to the ability to align the energy of terpyridine to E_F; however, the energy level of the metal itself is less important. We performed additional calculations on the Fe complex by using the same model. The β value of the Fe complex is 6.00×10^{-2} Å^{-1} (Figure 2), and the site-energy alignment is qualitatively the same as that of the Ru complex wire. To understand the electronic interaction between the terpyridine compound and the metal center, we estimated the charge donation between them by using the calculated density matrix. The donation of an (partial) electron from the metal to the terpyridine is observed in all of the studied complexes. However, the total charge donated by Ru and Fe centers is about 0.5 e larger than that from Cu. This difference originates from the d-electron of the metal atoms. The shift of the site energies of the terpyridine to E_F is caused by an additional electron occupation in the terpyridine orbital.

Next, we checked the profile of the transmission coefficient $\tau(E)$, which is a function of the electron energy E and sum of the major and minor spin components. The plots for Ru1L and Ru3L systems are shown in Figure 5. To clarify the resonance states relating to the distinct peaks, we performed a projected molecular orbital (PMO) analysis of the Ru1L system, in which the PMOs are the eigenstates of the MPSH matrix. Because we constructed an effective Hamiltonian, the complex energy is defined for each PMO φ_α. The real part is the MO energy ε_α, while the imaginary part consists of two terms γ_L and γ_R. These terms represent the "electronic coupling strengths" of each PMO with the left (γ_L) and right (γ_R) electrodes. The first-order contribution of the PMO φ_α to the resonance profile is identified by the Breit−Wigner formula as[28]

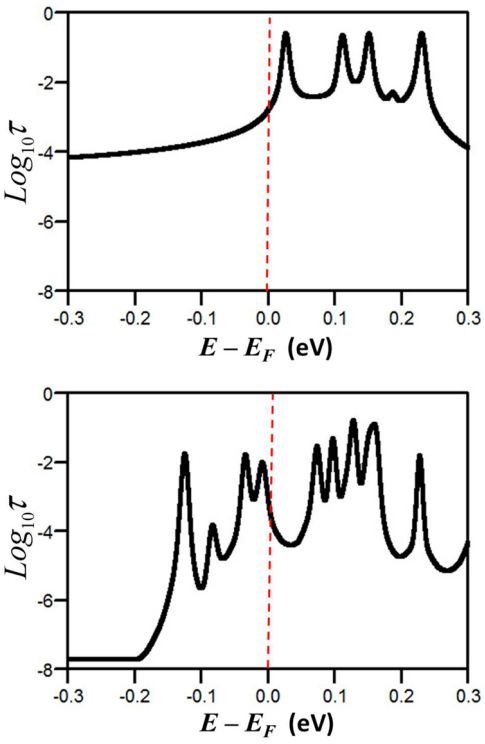

Figure 5. Log plot of the calculated transmission coefficient $\tau(E)$ as a function of energy. The upper and lower panels are relative to Ru1L and Ru3L, respectively.

$$\tau_\alpha = \frac{4\gamma_{\alpha L}\gamma_{\alpha R}}{(E_F - \varepsilon_\alpha)^2 + (\gamma_{\alpha L} + \gamma_{\alpha R})^2} \quad (1)$$

The electronic coupling strength and wave function plot of the PMOs of the major spin state of Ru1L are summarized in Figure 6. There are four nearly degenerate PMOs close to E_F

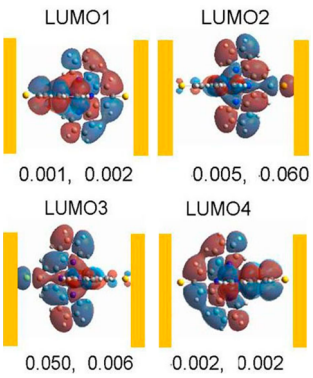

Figure 6. Spatial distribution of the projected molecular orbitals (PMOs) of Ru1L junctions. The electronic couplings with the left and right electrodes (in eV) are also shown for each PMO.

for both spin states within ∼0.2 eV, and all of the PMO energies are above E_F. The difference in the major and minor spin PMO energies is smaller than 0.05 eV. We refer to them as LUMO1−LUMO4. Even if the DFT error is included, the LUMO levels are closer to E_F than the HOMO level; thus, it is reasonable to conclude that the present four LUMOs dominate the tunneling. This result is consistent with other theoretical and experimental data on pyridine-based systems.[36]

dx.doi.org/10.1021/ja407662m | J. Am. Chem. Soc. XXXX, XXX, XXX−XXX

According to eq 1, contributions from the four LUMOs to the transport are not equivalent, and in comparison to LUMO1 and LUMO4, LUMO2 and LUMO3 dominate the electron tunneling because of the larger product between γ_L and γ_R. However, each resonance state is not an isolated resonance. For instance, the energy difference of neighboring PMOs in Ru1L is within ~0.05 eV, and these states can overlap. The interaction between each resonant state (off-diagonal element of H_{pp}) is so small that each resonance state can be identified by every φ_α; that is, they form weak overlapping resonances. From this PMO analysis, we concluded that the four comparable peaks in the $\tau(E)$ of Ru1L are related to the overlapping resonances of quasi-degenerated PMOs. Furthermore, the terms $\gamma_{L/R}$ depend on E [Supporting Information and eqs S4,S5]. According to these effects of energy dependence of γ and the overlap of resonances, each peak profile differs from that of a narrow isolated resonance. Usually, the charging effect by strong localization of a tunneling electron can be important when an electron passes an isolated narrow resonant state. On the contrary, in the present systems, an overlap of the resonance width forms the wide nonzero background in the transmission spectra. This non-Lorentzian profile makes the analysis by the NEGF-DFT approach possible, revealing that the tunneling time is faster than the possible trapped time in each resonant state; this theoretical consideration is consistent with the argument of the transport mechanism suggested by the previous experimental studies described above.[16,17] The most important factors for the following arguments about thermoelectricity are the small β and the control of the quantum resonance profile of $\tau(E)$ by linking many molecular units. By increasing the number of Ru complex units, the number of quasi-degenerate MOs is increased. Therefore, the number of narrow peaks should also increase, as confirmed by the finding that $\tau(E)$ of Ru3L has more overlapping peaks. Through interactions between the resonance states, some peak positions of Ru3L shift closer to E_F than those of Ru1L. In other words, the resonance peak positions are controlled by the number of the organometallic complex units, with more numerous units making $\tau(E)$ a more jaggy function.

3.2. Narrow Overlapping Resonance Effect on Thermopower and Lorentz Number. As discussed in the above section, overlapping resonances are controllable by increasing the number of organometallic molecular units. S_e is roughly estimated by the Mott formula, $S_e \propto T(\partial \ln \tau)/(\partial E)|_{E_F}$, and the cusp shoulder at $E \approx E_F$ of a nodal/jaggy $\tau(E)$ gives a large S_e. On this basis, the enhancement of S_e has been proposed for several single-molecular junctions,[9] where nodal $\tau(E)$ is presented by controlling the Fano resonance. The Fano profile of $\tau(E)$ can be found in molecular junctions when continuum (tunneling) and bound (localized) states are moderately mixed by interferences. In most cases, the continuum and bound states depend on the electronic states of the π-conjugated backbone and side group, respectively. The designed molecules are sometimes called cross-conjugated molecules.[8−11,37−39] In addition to searching promising side groups, the optimization of electrodes and nanostructured materials was discussed.[40] On the contrary, the narrow overlapping resonance is the interference of the weakly interacting quasi-degenerate tunneling states.[41]

As predicted by the first-principles calculations, narrow overlapping resonances by quasi-degenerate MOs are responsible for the long-range transport of organometallic complexes. The plot of $\tau(E)$ of the Ru complex becomes multipeaked jaggy, and some of their shoulders (or cusps) move toward E_F. Therefore, a larger S_e than that of the usual off-resonant or broad-resonant tunneling systems is expected. We compared the temperature dependence of S_e of the Ru1L and Ru3L junctions. S_e is obtained by using the Onsager coefficients $L_{(0)}$ and $L_{(1)}$.

$$S_e = -\frac{1}{T}\frac{L^{(1)}}{L^{(0)}} \tag{2}$$

The nth-order coefficient $L^{(n)}$ is defined as

$$L^{(n)} = \frac{1}{2\pi}\int \mathrm{d}E\left(-\frac{\partial f(E,T)}{\partial E}\right)(E - E_F)^n \tau(E) \tag{3}$$

where f is the Fermi function. The calculated S_e is plotted as a function of temperature in Figure 7. S_e is proportional to L for

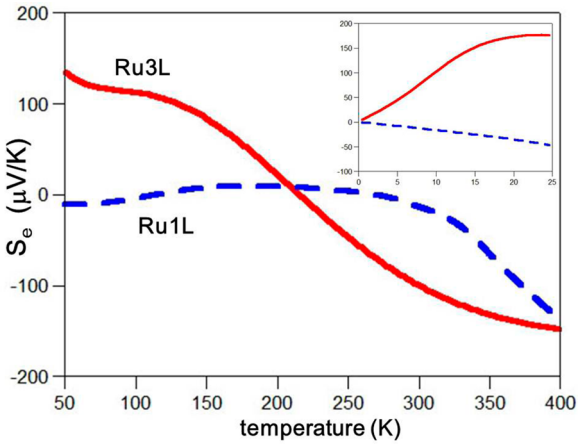

Figure 7. Plots of the Seebeck coefficient (S_e) of Ru1L and Ru3L as functions of temperature in the 50−400 K range. The blue dashed and red solid lines represent the plots of Ru1L and Ru3L, respectively. Inset: Plots in the temperature zone below 25 K. In the limit of $T \to 0$, S_e approaches zero.

standard organic molecular wires; however, this does not apply to Ru complex. From the viewpoint of material design, our approach and the use of the Fano resonance are very different; that is, the former is realized by optimizing the number of molecular units (e.g., assembling), while the latter requires chemical modification of the side groups. The temperature dependence of S_e in Ru3L is more distinctive. S_e is a monotonically decreasing function of the temperature and changes its sign at ~220 K. The distinct sign change of S_e is triggered by two or more narrow peaks of τ located close to each other as well as to E_F.

The large thermopower is obtained by enhancing S_e; however, the efficiency of thermoelectric conversion is characterized by ZT, which is defined as $ZT = (\sigma S_e^2)/\kappa$, where κ is the thermal conductance. When the phonon effect is neglected, the electric and thermal conductance are represented as

$$\sigma = L^{(0)} \tag{4}$$

$$\kappa_e = \frac{1}{2\pi}\left(L^{(2)} - \frac{(L^{(1)})^2}{L^0}\right) \tag{5}$$

dx.doi.org/10.1021/ja407662m | J. Am. Chem. Soc. XXXX, XXX, XXX−XXX

where the thermal conductance term is rewritten as κ_e, and thus $Z_eT = (\sigma S_e^2)/\kappa_e$. At first glance, three strategies appear to achieve a large Z_eT: (i) enhancing S_e, (ii) increasing σ, and (iii) suppressing κ_e. However, strategies (ii) and (iii) would be difficult because the modulation of σ and κ cannot be achieved independently if the WF law is satisfied, which states that the Lorentz number ($L_Z \equiv \kappa_e/\sigma T$) is constant. The constant value (WF constant, L_{WF}) is equal to $(\pi^2 k_B)/3$ for noninteracting systems, where k_B is the Boltzmann constant. However, recent theoretical analyses have proved that the WF law can fail in mesoscopic conductors[42] or small molecular wires.[43,44] A previous study[44] states the validity of the WF law by considering the energy integral of the Onsager coefficients. When the sharpness of the function $(\partial f)/(\partial E)$ is comparable to that of the resonance peaks of $\tau(E)$, the jaggy $\tau(E)$ is not simply averaged, and thus the WF law will be violated.[12,43] Because the $\tau(E)$ of Ru3L satisfies the above condition, the deviation from the WF law is expected. However, the violation of the WF law can provide both larger and smaller L_Z than L_{WF}. Large L_Z eliminates the advantage of large S_e because Z_eT is expressed as $Z_eT = (S_e^2)/L_Z$; thus, it is useful to check whether L_Z is in the preferred/reasonable range ($L_z/L_{WF} \ll 1$, $1 \approx L_z/L_{WF}$). The calculated Lorentz number $L_Z(T)$ and Z_eT are given in Figure 8a and b, respectively. The WF law holds for Ru1L up to 300 K because the resonance positions are ~0.04 eV above E_F, even though their sharpness is sufficiently comparable to that of $(\partial f)/(\partial E)$ at $T \geq 50$ K. On the contrary, deviation from the WF law is found clearly for Ru3L in the focused temperature region of 50−400 K. In particular, L_Z is lower than L_{WF} at $T \approx 150$ K. The maximum value of L_Z is $2L_{WF}$, and hence the deviation from the WF law does not significantly suppress Z_eT.

S_e is proportional to L, and L_Z is independent of L; thus, Z_eT is approximately proportional to L^2 for standard molecular/atomic wires.[45] On the contrary, Z_eT of Ru complex can be more rapidly increased than L^2 because of the jaggy profile of $\tau(E)$. Note that the efficiency of the thermoelectricity strongly depends on the working temperature of the device according to a strong temperature dependence of S_e. A sign change of S_e and zero ZT in the specific temperature region are the distinct features of thermoelectric materials via overlapping resonance.

3.3. Figure of Merit and Effects of Phonon Thermal Transport. Finally, we considered the effects of phonon thermal transport on ZT. When the electron−phonon interaction is neglected, the thermal conductance κ is represented by the sum of the electric and phonon thermal conductances, that is, $\kappa = \kappa_e + \kappa_{ph}$. Assuming that phonon transport is ballistic in the wire, the phonon heat flux is expressed by the phonon transmission coefficient $\tau_{ph}(\omega)$ as

$$J = \frac{1}{2\pi}\int d\omega\, \omega\tau_{ph}(\omega)(N_L^{BE} - N_R^{BE}) \quad (6)$$

where $N_{L(R)}^{BE}$ is the Bose−Einstein function at $T = T_{L(R)}$. The phonon thermal conductance is defined as a function of the average temperature T:

$$\kappa_{ph} = \frac{1}{2\pi}\int d\omega\, \omega\frac{\partial N^{BE}(\omega, T)}{\partial T}\tau_{ph}(\omega) \quad (7)$$

We adopted a weak-link approximation[46] to calculate τ_{ph}, while the surface phonon Green's functions of the electrodes were rigorously calculated by DFT. Next, the Green's functions were assembled into a finite contact region. Therefore, anisotropic effects of the finite contact region and surface structure (e.g., the effects of the transverse and longitudinal surface modes and the surface Miller index) are included in the present calculation of τ_{ph}.

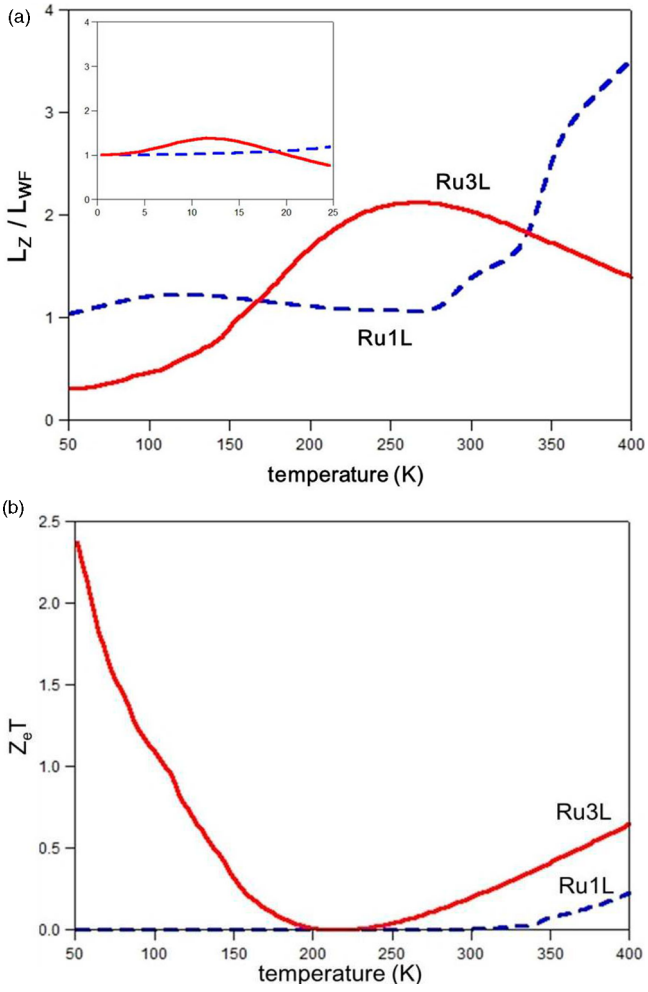

Figure 8. (a) Lorentz number and (b) figure of merit calculated by omitting the phonon effect of Ru1L and Ru3L wires plotted as functions of temperature in the 50−400 K range. The blue dashed and red solid lines represent the plots of Ru1L and Ru3L wires, respectively. The Lorentz number is normalized by the Wiedemann−Franz (WF) constant. Inset (a) highlights the Lorentz number in the temperature zone below 25 K. In the limit of $T \to 0$, the Lorentz number approaches the WF constant.

Figure 9a shows the resulting phonon thermal conductance of Ru1L and Ru3L. The raising part of κ_{ph} is slightly more gentle than the power law ($\kappa_{ph} \propto T^3$) even though the temperature is lower than the Debye temperature ($T < 100$ K) due to anisotropy by bulk termination.[45] The monotonous decrease in κ_{ph} as a function of L corresponds to the decrease in stiffness. For comparison, we calculated κ_{ph} of Cu3L. When the wire is strained, deformation of the Cu complex is larger than that of the Ru complex. As a result, the change in the energy of Cu complex is larger by the same strain value. The calculated stiffness of Cu3L is 2.1 times larger than that of Ru3L. The plots of ZT including κ_{ph} are given in Figure 9b for Ru1L, Ru3L, and Cu3L. We found that ZT becomes much smaller than the corresponding Z_eT in all cases, but in particular for $T \leq 100$ K. To analyze the length dependence of ZT upon phonon effects, we rewrite ZT as

dx.doi.org/10.1021/ja407662m | J. Am. Chem. Soc. XXXX, XXX, XXX−XXX

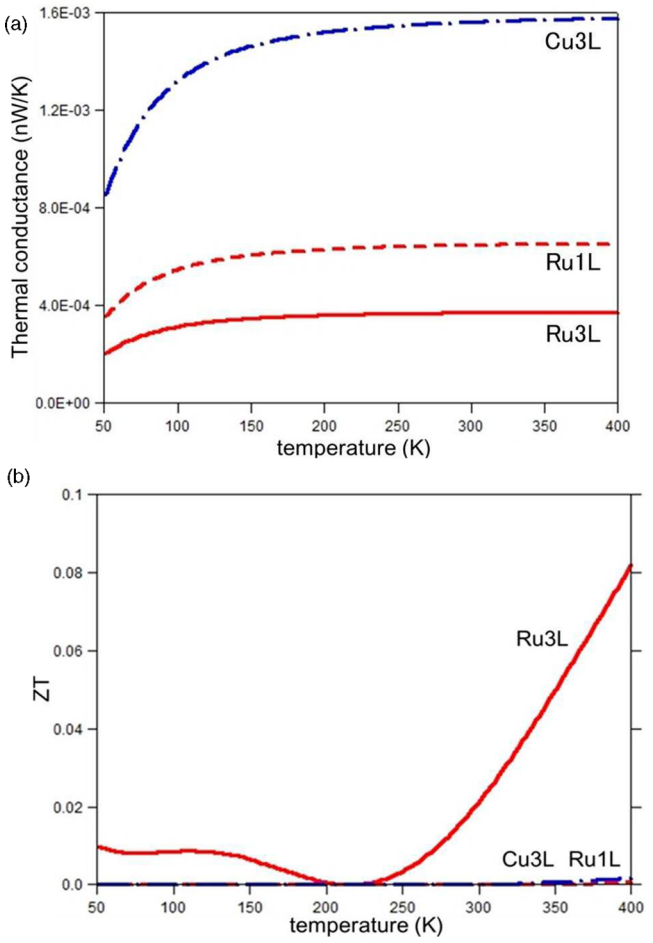

Figure 9. (a) Phonon thermal conductivity and (b) figure of merit of Cu3L, Ru1L, and Ru3L wires. All plots are given as functions of temperature. The blue dashed and dotted, red dotted, and red solid lines represent the results of Cu3L, Ru1L, and Ru3L wires, respectively.

$$ZT = \frac{Z_e T}{1 + \kappa_{ph}/\kappa_e} = \frac{Z_e T}{1 + \tilde{\kappa}} \tag{8}$$

The calculated $\tilde{\kappa}$ of Ru1L and Cu1L are 4.0×10^4 and 2.2×10^7 at low temperatures (~50 K), while they are 5.6×10^2 and 2.6×10^3 at high temperatures (~350 K), respectively. $\tilde{\kappa}$ of the Cu complex wire increases more rapidly than that of the Ru complex wire as a function of L because the length dependence of $\tilde{\kappa}$ is approximated as $\tilde{\kappa} \propto L^{-2} \exp(\beta L)$ at low temperatures. Because of this slow increase and a large Z_eT, Ru3L has a ZT significantly larger than zero. Because κ_{ph} assumes an almost constant value as a function of temperature in the high-temperature region, the temperature dependence of $\tilde{\kappa}$ is dominated by κ_e at high temperatures. Similar to Z_eT, ZT of Ru3L clearly increases above 250 K and reaches ~0.05 at 350 K. However, κ_{ph} is still much larger than κ_e, and ZT of Ru3L reduced to 11% of Z_eT at 400 K by phonon thermal effect.

Here, we emphasize that in comparison to a single unit, a wire lengthened by the organometallic molecular units better improves ZT; that is, (i) large S_e is achieved by narrow overlapping resonances and (ii) the rapid decrease in ZT because of the relatively increased phonon effect caused by the lengthening of the wire is suppressed by a small β. In addition, in the field of phonon engineering, phonon mismatching between the electrode phonon and internal vibrational modes of molecules is expected. Several ZT of organic molecular materials have been reported; however, these materials are either conducting polymers or composite systems.[47,48] Their ZT values are typically 0.1−0.2 at room temperature, which is similar to the value obtained for our Ru3L system; thus, our simulation predicts that an organometallic molecular material is an alternative promising candidate for thermoelectric circuits of organic compounds.

4. CONCLUSIONS

We studied the role of metal centers in superior long-range electric transport of organometallic molecular wires by means of first-principles calculations. We adopted terpyridine-based complexes as computational model systems. We observed that quasi-resonant tunneling is mediated by organic compounds. First-principles calculations predict that incorporated d-electron metals such as Ru drastically improve the site-energy alignment of organic compounds by charge donation. A complex molecular unit has quasi-degenerated MOs that form overlapping resonances when the unit is used for lengthening a wire; the transfer integrals between the units are so small that their resonance are weakly overlapping. This length-dependent resonance profile prevents a rapid decrease of conductance allowing for small β. The jaggy profile of the transmission coefficient is practically achieved by lengthening the molecular wire (i.e., by increasing the number of organometallic molecular units).

Controlling overlapping resonances is an alternative approach to use the Fano profile for increasing ZT by quantum effect. The jaggy profile of the transmission coefficient can be controlled by optimizing the wire length; moreover, it enhances the Seebeck coefficient and/or provides the violation of the WF law. For the studied Ru complexes, the Seebeck coefficient is a monotonically decreasing function in the focused temperature region that changes its sign. The results show that ZT is almost zero in the limited-temperature region. Shifting this specific temperature from the target temperature of the device is an interesting MO engineering problem.

The effect of phonon thermal transport was considered in the weak-link mode with the explicit calculation of phonon self-energies. ZT is reduced by phonon thermal transport. However, because of a small β value, the length dependence of the phonon thermal effect on ZT is suppressed. This is another advantage of organometallic wires. To develop high-ZT materials using organometallic molecules, further careful design of MOs and anchors is required. This will be possible by designing conducting MOs satisfying the symmetric electronic coupling strength with left and right electrodes.[16,28] A promising approach is to design a π-contact multiple-leg anchor for organometallic molecular units such as a tripodal pyridine moiety.[29]

■ ASSOCIATED CONTENT

Ⓢ Supporting Information

Theoretical methods and computations, and additional references. This material is available free of charge via the Internet at http://pubs.acs.org.

■ AUTHOR INFORMATION

Corresponding Author

hs-nakamura@aist.go.jp

dx.doi.org/10.1021/ja407662m | J. Am. Chem. Soc. XXXX, XXX, XXX−XXX

Notes

The authors declare no competing financial interest.

■ ACKNOWLEDGMENTS

H.N. is grateful to the Cooperative Research Program of "Network Joint Research Center for Materials and Devices" and for the financial support provided by the Scientific Research on Innovative Areas, a MEXT Grant-in-Aid Project: "Materials Design through Computics" (#25104724). H.N. and Y.A. are thankful for the Grant-in-Aid for Scientific Research on Innovation Areas "Molecular Architectonics: Orchestration of Single Molecules for Novel Functions" (#25110009).

■ REFERENCES

(1) Briseno, A. L.; Mannsfeld, S. C. B.; Ling, M. M.; Liu, S. H.; Tseng, R. J.; Reese, C.; Roberts, M. E.; Yang, Y.; Wudl, F.; Bao, Z. N. *Nature* **2006**, *444*, 913.
(2) Chen, J.; Wang, W.; Klemic, J.; Reed, M. A.; Axelrod, B. W.; Kaschak, D. M.; Rawlett, A. M.; Price, D. W.; Dirk, S. M.; Tour, J. M.; Grubisha, D. S.; Bennett, D. W. *Ann. N. Y. Acad. Sci.* **2002**, *960*, 69.
(3) Aviram, A.; Ratner, M. A. *Chem. Phys. Lett.* **1974**, *29*, 277.
(4) Ellenbogen, J. C.; Love, J. C. *Proc. IEEE* **2000**, *88*, 386.
(5) Heimel, G.; Zojer, E.; Romaner, L.; Bredas, J. L.; Stellacci, F. *Nano Lett.* **2009**, *9*, 2559.
(6) Malen, J. A.; Yee, S. K.; Majumdar, A.; Segalman, R. A. *Chem. Phys. Lett.* **2010**, *491*, 109.
(7) Papadopoulos, T. A.; Grace, I. M.; Lambert, C. J. *Phys. Rev. B* **2006**, *74*, 193306.
(8) Bergfield, J. P.; Stafford, C. A. *Nano Lett.* **2009**, *9*, 3072.
(9) Finch, C.; García-Suárez, V.; Lambert, C. *Phys. Rev. B* **2009**, *79*, 033405.
(10) Andrews, D. Q.; Solomon, G. C.; Goldsmith, R. H.; Hansen, T.; Wasielewski, M. R.; Van Duyne, R. P.; Ratner, M. A. *J. Phys. Chem. C* **2008**, *112*, 16991.
(11) Ke, S.-H.; Yang, W.; Curtarolo, S.; Baranger, H. U. *Nano Lett.* **2009**, *9*, 1011.
(12) Asai, Y.; Fukuyama, H. *Phys. Rev. B* **2005**, *72*, 085431.
(13) Luo, L.; Benameur, A.; Brignou, P.; Choi, S. H.; Rigaut, S.; Frisbie, C. D. *J. Phys. Chem. C* **2011**, *115*, 19955.
(14) Nishimori, Y.; Kanaizuka, K.; Kurita, T.; Nagatsu, T.; Segawa, Y.; Toshimitsu, F.; Muratsugu, S.; Utsuno, M.; Kume, S.; Murata, M.; Nishihara, H. *Chem.-Asian J.* **2009**, *4*, 1361.
(15) Sedghi, G.; Garcia-Suarez, V. M.; Esdaile, L. J.; Anderson, H. L.; Lambert, C. J.; Martin, S.; Bethell, D.; Higgins, S. J.; Elliott, M.; Bennett, N.; Macdonald, J. E.; Nichols, R. J. *Nat. Nanotechnol.* **2011**, *6*, 517.
(16) Terada, K.-i.; Nakamura, H.; Kanaizuka, K.; Haga, M.-a.; Asai, Y.; Ishida, T. *ACS Nano* **2012**, *6*, 1988.
(17) Tuccitto, N.; Ferri, V.; Cavazzini, M.; Quici, S.; Zhavnerko, G.; Licciardello, A.; Rampi, M. A. *Nat. Mater.* **2008**, *8*, 41.
(18) Mahapatro, A. K.; Ying, J. W.; Ren, T.; Janes, D. B. *Nano Lett.* **2008**, *8*, 2131.
(19) Holstein, T. *Ann. Phys.* **1959**, *8*, 343.
(20) Asai, Y. *Phys. Rev. B* **2011**, *84*, 085436.
(21) Matsuhita, R.; Horikawa, M.; Naitoh, Y.; Nakamura, H.; Kiguchi, M. *J. Phys. Chem. C* **2013**, *117*, 1791.
(22) Jauho, A. P.; Wingreen, N. S.; Meir, Y. *Phys. Rev. B* **1994**, *50*, 5528.
(23) Keldysh, L. V. *Sov. Phys.-JETP* **1965**, *20*, 1018.
(24) Nakamura, H.; Yamashita, K. *J. Chem. Phys.* **2006**, *125*, 194106.
(25) Nakamura, H.; Yamashita, K.; Rocha, A. R.; Sanvito, S. *Phys. Rev. B* **2008**, *78*, 235420.
(26) Cresti, A.; Farchioni, R.; Grosso, G.; Parravicini, G. P. *Phys. Rev. B* **2003**, *68*, 075306.
(27) Nakamura, H. *J. Phys. Chem. C* **2010**, *114*, 12280.
(28) Nakamura, H.; Asai, Y.; Hihath, J.; Bruot, C.; Tao, N. *J. Phys. Chem. C* **2011**, *115*, 19931.
(29) Ie, Y.; Hirose, T.; Nakamura, H.; Kiguchi, M.; Takagi, N.; Kawai, M.; Aso, Y. *J. Am. Chem. Soc.* **2011**, *133*, 3014.
(30) Kamenetska, M.; Quek, S. Y.; Whalley, A. C.; Steigerwald, M. L.; Choi, H. J.; Louie, S. G.; Nuckolls, C.; Hybertsen, M. S.; Neaton, J. B.; Venkataraman, L. *J. Am. Chem. Soc.* **2010**, *132*, 6817.
(31) Li, R.; Hou, S. M.; Zhang, J. X.; Qian, Z. K.; Shen, Z. Y.; Zhao, X. Y. *J. Chem. Phys.* **2006**, *125*, 194113.
(32) Quek, S. Y.; Choi, H. J.; Louie, S. G; Neaton, J. B. *Nano Lett.* **2009**, *9*, 3949.
(33) Thygesen, K. S. *Phys. Rev. Lett.* **2008**, *100*, 166804.
(34) Thygesen, K. S.; Rubio, A. *Phys. Rev. B* **2008**, *77*, 115333.
(35) Toher, C.; Sanvito, S. *Phys. Rev. B* **2008**, *77*, 155402.
(36) Widawsky, J. R.; Darancet, P.; Neaton, J. B.; Venkataraman, L. *Nano Lett.* **2012**, *12*, 354.
(37) Pauly, F.; Viljas, J.; Cuevas, J. *Phys. Rev. B* **2008**, *78*, 035315.
(38) Murphy, P.; Mukerjee, S.; Moore, J. *Phys. Rev. B* **2008**, *78*, 161406.
(39) Solomon, G. C.; Andrews, D. Q.; Goldsmith, R. H.; Hansen, T.; Wasielewski, M. R.; Van Duyne, R. P.; Ratner, M. A. *J. Am. Chem. Soc.* **2008**, *130*, 17301.
(40) Nozaki, D.; Sevinçli, H.; Li, W.; Gutiérrez, R.; Cuniberti, G. *Phys. Rev. B* **2010**, *81*, 235406.
(41) Polik, W. F.; Moore, C. B.; Miller, W. H. *J. Chem. Phys.* **1988**, *89*, 3584.
(42) Vavilov, M. G.; Stone, A. D. *Phys. Rev. B* **2005**, *72*, 205107.
(43) Asai, Y. *J. Phys.: Condens. Matter* **2013**, *25*, 155305.
(44) Balachandran, V.; Bosisio, R.; Benenti, G. *Phys. Rev. B* **2012**, *86*, 035433.
(45) Liu, Y.-S.; Chen, Y.-R.; Chen, Y.-C. *ACS Nano* **2009**, *3*, 3497.
(46) Patton, K.; Geller, M. *Phys. Rev. B* **2001**, *64*, 155320.
(47) Bubnova, O.; Crispin, X. *Energy Environ. Sci.* **2012**, *5*, 9345.
(48) Bubnova, O.; Khan, Z. U.; Malti, A.; Braun, S.; Fahlman, M.; Berggren, M.; Crispin, X. *Nat. Mater.* **2011**, *10*, 429.